Beyond endocrine resistance: estrogen receptor (ESR1) activating mutations mediate chemotherapy resistance through the JNK/c-Jun MDR1 pathway in breast cancer

Marwa Taya (marwa.taya@gmail.com)
Department of Oncology, Tel Aviv Sourasky Medical Center, Tel Aviv

Keren Merenbakh-Lamin
Department of Oncology, Tel Aviv Sourasky Medical Center, Tel Aviv

Asia Zubkov
Institute of Pathology, Tel Aviv Sourasky Medical Center, Tel Aviv

Zohar Honig
Department of Oncology, Tel Aviv Sourasky Medical Center, Tel Aviv

Alina Kurolap
The Genetics Institute and Genomics Center, Tel Aviv Sourasky Medical Center, Tel Aviv

Ori Mayer
Faculty of Medicine, Tel Aviv University, Tel Aviv

Noam Shomron
Faculty of Medicine, Tel Aviv University, Tel Aviv

Ido Wolf
Department of Oncology, Tel Aviv Sourasky Medical Center, Tel Aviv

Tami Rubinek
Department of Oncology, Tel Aviv Sourasky Medical Center, Tel Aviv

Research Article

Keywords: Chemoresistance, activating mutations, MDR1, JNK/c-Jun signaling pathway, JNK inhibitor

Posted Date: January 12th, 2024

DOI: https://doi.org/10.21203/rs.3.rs-3833915/v1

Additional Declarations: No competing interests reported.

Abstract

Purpose

All patients with metastatic breast cancer (MBC) expressing estrogen receptor-α (ESR1) will eventually develop resistance to endocrine therapies. In up to 40% of patients, this resistance is caused by activating mutations in the ligand-binding domain (LBD) of ESR1. Accumulating clinical evidence indicate adverse outcomes for these patients, beyond that expected by resistance to endocrine therapy. We hypothesized that ESR1 mutations may also confer resistance to chemotherapy.

Experimental Design:

MCF-7 cells harboring Y537S and D538G ESR1 mutations (mut-ER) were employed to study response to chemotherapy using viability and apoptotic assay in vitro, and tumor growth in vivo. JNK/c-Jun/MDR1 pathway was studied using qRT-PCR, western-blot, gene-reporter and ChIP assays. MDR1 expression was analyzed in clinical samples using IHC.

Results

Cell harboring ESR1 mutations displayed relative chemoresistance, evidenced by higher viability and reduced apoptosis as well as resistance to paclitaxel in vivo. To elucidate the underlying mechanism, MDR1 expression was examined and elevated levels were observed in mut-ER cells, and in clinical BC samples. MDR1 is regulated by the JNK/c-Jun pathway, and indeed, we detected higher JNK/c-Jun expression and activity in mut-ER cells, as well as increased occupancy of c-Jun in MDR1 promoter. Importantly, JNK inhibition decreased MDR1 expression, particularly of D538G-cells, and reduced viability in response to chemotherapy.

Conclusions

Taken together, these data indicate that ESR1 mutations confer chemoresistance in BC through activation of the JNK/MDR1 axis. Targeting this pathway may restore sensitivity to chemotherapy and serve as a novel treatment strategy for MBC patients carrying ESR1 mutations.

Introduction

Breast cancer (BC) is the most frequently diagnosed malignancy and the leading cause of cancer related death among women[1]. About 75% of patients with BC express estrogen receptor-α (ESR1) and endocrine therapy is the mainstay treatment for these patients. While being effective and safe, some patients with metastatic breast cancer (MBC) do not respond to any form of endocrine treatment (de novo resistance),

and virtually all patients who initially respond will eventually develop endocrine resistance (acquired resistance)[2]. We and others have discovered activating mutations in the ligand binding domain (LBD) of the ESR1 as an acquired mechanism for endocrine resistance[2–6], with D538G and Y537S being the most common mutations[7–9]. These mutations arise following endocrine treatment, most commonly aromatase inhibitors, and are identified in up to 40% of patients with ER-positive MBC [7,8,10].

Accumulating clinical and laboratory data suggest a unique aggressive phenotype of BC expressing these mutations beyond merely endocrine resistance. Thus, we and others have shown predilection of tumors and cells harboring these mutations to form liver metastasis[2,11,12]. Moreover, these data indicates that following the development of endocrine resistance, the outcomes for patients with tumors harboring ESR1 mutations are significantly worse compared to those with other forms of endocrine resistance [7,8,13].

Following the development of endocrine resistance, patients with MBC are treated with chemotherapy, paclitaxel and doxorubicin are being among the most commonly used agents [14]. Yet, some patients rapidly develop resistance to these agents as well. Mechanisms associated with resistance to chemotherapy include the activation of survival pathways, such as PI3K/AKT/mTOR, and alterations in drug metabolism, including drug uptake, efflux, and detoxification[15].

Multiple Drug Resistance (MDR) refers to the ability of cancer cells to resist a variety of chemotherapeutic drugs. The MDR phenotype occurs most often due to the overexpression of drug efflux pumps in the plasma membrane of cancer cells[16], including the multi-drug resistance 1 (MDR1) gene, which is known as ABCB1. It encodes an efflux transporter that limits drugs from penetrating cells and depositing them into the extracellular space[17]. Expression of MDR1 was noted in over 50% of cancers with MDR phenotype and it can be inherited or induced by chemotherapy[18]. A well-established regulator of the MDR phenotype is c-Jun NH2-terminal kinase (JNK) pathway. Exposure of tumors to chemotherapy activates JNK [19], leading to phosphorylation and activation of its downstream effector, the transcription factor c-Jun [20], which in turn upregulates the expression of MDR1 [21,22].

Based on the accumulating clinical data, we hypothesized that ESR1 activating mutations confer resistance to chemotherapy. Indeed, our results indicate an association between these mutations and resistance to chemotherapy in BC cells. Furthermore, MDR1 was upregulated in mut-ER, especially in D538G-ER, and this was associated with increased activity of the JNK/c-Jun pathway. Importantly, inhibition of this pathway increased sensitivity to doxorubicin. These data suggest a novel treatment strategy for patients harboring activating ESR1 mutations.

Materials and Methods

Chemicals and reagents

Paclitaxel (Taxol; 6mg/ml) and doxorubicin (2mg/ml) were provided from the pharmacy of the Oncology department at Sourasky Medical Center (Tel Aviv, Israel). SP600125 (10mg) ≥ 98% HPLC and JNK inhibitor X (BI-78D3; 5mg) were purchased from Sigma- Aldrich (St. Louis, MO, USA).

Cells

Cell lines were originally obtained from the American Type Culture Collection (ATCC) and authenticated with the DNA markers used by ATCC. MCF-7 and T47D cells were grown in Dulbecco's Modified Eagle's Medium (DMEM) containing 10% fetal bovine serum (FBS). MCF-7 cell lines stably expressing WT-ER, D538G-ER, and Y537S-ER, were generated in the lab using lentiviral infection[2,12].

Methylene blue assay

Viability and proliferation were assessed using methylene blue assay as previously described[12]. For this assay, cells (WT-ER, D538G, or Y537S expressing cells) were plated in 96-well plates at a density of 5000 cells per well and treated with various concentrations of chemotherapy drugs (10 wells per treatment) for 72 hours. To end the assay, glutaraldehyde (2.5%) was dilute 1:5 into cells for 10 min and then cells were washed three times with ddH_2O. Cells were incubated with 100µl of methylene blue stain [1% methylene blue in borate buffer (pH 8.5)] for 1 hour at room temperature. After removing the methylene blue stain, cells were washed with dH_2O to completely remove the stain and 100µl of 0.1M HCl was added into each well following dryness. The absorbance was read with a microplate reader at 650nm.

Colony assay

Cells were cultured at low density (1500 cells/well) in 6–well plates and were treated twice a week with different concentrations of chemotherapies (0.5nM paclitaxel, 5nM doxorubicin). After two weeks, cells were fixed and stained with 0.01% crystal violet diluted with 95% ethanol for 40 minutes. Quantification of colonies was done by dissolving in 10% acetic acid and read in a plate reader at 560nm wavelength.

Luciferase assay

Cells were seeded in 12-well plates and transfected with the AP-1 reporter vector (3XAP1PGL3). Luciferase assay was conducted using the Luciferase Assay System kit (Promega, CA) according to the manufacturer's instructions. Luciferase units were normalized to protein concentration.

Apoptosis assay

For the cell cycle and apoptosis analyses, cells were evaluated by measuring 7AAD and Annexin-FITC V staining using fluorescence-activated cell sorter (FACS Caliber Becton Dickinson). Apoptosis was determined by flow cytometry analysis using annexin-V FITC in accordance with the manufacturer’s instructions (Invitrogen). Briefly, after treatment, adherent cells were harvested and resuspended in 200µL binding buffer containing 5µL of annexin-V fluorescein isothiocyanate and 5µL of 7AAD, then incubated for 15 minutes in the dark at room temperature. Analysis was immediately performed using flow cytometer. Data was analyzed by FlowJo software.

Quantitative RT-PCR

Genes expression was evaluated as previously stated[12]. Briefly, the total RNA was extracted using the High Pure RNA Isolation Kit (Roche). Total RNA (1µg) was reverse transcribed using qScript cDNA synthesis kit (Quanta Biosciences). Quantitative RT-PCR (qRT-PCR) was used to determine mRNA level. Primers were synthesized by IDT (Coralville, IA, USA). Amplification reactions were performed with Platinum qPCR SuperMix in triplicate using StepOne Plus (Applied Biosystems). PCR conditions: 50°C for 2 min, 95°C for 2 min, followed by 40 cycles of 95°C for 15 sec, 60°C for 45 sec. The primer sequences for the genes were as follows: MDR1: F- TTCAACTATCCCACCCGACCGGAC, R- ATGCTGCAGTCAAACAGGATGGGC; c-Jun: F- CAGCCAGGTCGGCAGTATAG, R- GGGACTCTGCCACTTGTCTC; β-actin: F- GCTCAGGAGGAGCAATGATCTT; R- TTGCCGACAGGATGCAGAA.

Western blot

Cells were harvested, lysed, and the total protein was extracted with radioimmunoprecipitation assay (RIPA) buffer (50mM Tris–HCl pH 7.4, 150mM NaCl, 1% NP-40,0.25% Na-deoxycholate, 1mM EDTA, 1mM NaF), together with a protease and phosphatase inhibitor cocktails (Sigma). Lysates were resolved on 10% SDS-PAGE and immunoblotted with the indicated antibodies:

β-actin (A5441; sigma, St. Louis, MO); p-JNK (AF1205; R&D systems, Minneapolis, United States), p-c-Jun (ser73) (cat# 3270;cell signaling, Massachusetts, United States), T-JNK (cat# 9252;cell signaling, Massachusetts, United States), anti P-glycoprotein (ab170904; Abcam, Cambridge, United Kingdom), T-ERK (M-5670; Sigma, St. Louis, MO), c-PARP (cat# 5625; cell signaling, Massachusetts, United States)

Chromatin immunoprecipitation (ChIP) assay

The assay was performed using Magna ChIP A/G Kit (EMD Millipore Corporation). Cells were grown in 150 mm plates and cross- linked with 1% formaldehyde. Following sonication, chromatin was immunoprecipitated overnight with c-Jun antibody (60A8; Cell Signaling). Normal rabbit IgG (Jackson ImmunoResearch Laboratories, INC) was used as a control. Total DNA was extracted and samples were analyzed on 1.5% agarose after 30 cycles of PCR amplification with primers spanning the AP-1 site on MDR1 promoter: (F) 5’ CCTCCTGGAAATTCAACCTTG-3’, (R) 5’-GAAGAGCCGCTAGAATG-3’ as previously studied[23]

Immunohistochemistry (IHC)

The slides were deparaffinized in xylene (Bio-Lab ltd) and rehydrated in graded concentrations of alcohol. Antigen retrieval was performed using a 10mM sodium citrate buffer solution at pH 6.0. Sections were placed in a 3% hydrogen peroxide for 30 minutes to quench any endogenous peroxidase activity, followed by several washes of PBS with Tween 20 (PBST) and then incubated with normal horse serum 2.5% (ImmPRESS universal polymer kit peroxidase) for 20 minutes. Then, the slides were incubated with primary antibody which was diluted with an antibody diluent (Zytomed Systems) overnight. Antibodies used: anti p-JNK (R&D cat# AF1205; 1:100) and P-gp (abcam cat#ab170904; 1:100). Next, slides were

incubated with horseradish peroxidase (HPR) for 30 minutes followed by two washes of PBS with Tween 20 (PBST) and stained with diaminobenzidine (DAB) (ImmPACT DAB Kit) and hematoxylin (Merck). For quantification, number of p-JNK and P-gp cells per field, 4 fields per group, were determined using ImageJ. The P-gp score in patients' clinical samples was interpreted on the basis of percentage of positive cells against total population of cells as previously described[24].

Intracellular accumulation of doxorubicin

Confocal microscopic observation. MCF-7 cells stably expressing WT-ER and D538G were seeded at a density of 50,000 cells onto the coverslips of 12-well plates. After 24 hours, cells were treated with 10μM doxorubicin alone or in combination with SP600125 (20μM) for 3 hours. Cells were fixed with 4% paraformaldehyde in PBS for 10 minutes, followed by three washes with PBS. Then cells were permeabilized with 0.1% Triton X-100 in PBS for 5 minutes at room temperature and followed by three washes of PBS, 10 minutes each. After blocking with CAS-Block (Invitrogen), cells were stained with anti-EpCAM antibody (abcam, 1:500 diluted with CAS-Block) overnight at 4°C. After three washes with PBS, the sections were incubated with goat anti-rabbit AlexaFluor 488 antibody (Jackson ImmunoResearch Laboratories, 1:200 dilution) for 1 hour at room temperature. Following three washes with PBS, 4,6-diamidino-2-phenylindole (DAPI) (Rhenium) was added for two minutes, followed by two washes with PBS. The coverslips were wet-mounted using Fluoromount aqueous mounting (Sigma) on microscope slides. Slides were observed under LSM 700 confocal laser scanning microscope (Zeiss, Germany) using the 40X magnification.

Flow cytometry. To quantify the intracellular accumulation of doxorubicin, WT-ER and D538G cells were seeded in 6 well plates. After 24 hours, cells were treated with 10μM doxorubicin alone or in combination with SP600125 (20μM) for 24 hours. The control samples were incubated without any treatment. Then, samples were washed twice with PBS, harvested, and the fluorescence intensity was determined using flow cytometry (FACScantoII; Becton Dickinson, NJ, USA). A minimum of 10,000 events were collected for each sample. The data were analyzed with FlowJo software. The fluorescence intensity was expressed as Geometric Mean.

Patients clinical data and Tumor Specimens

Tumor samples were provided in the form of formalin-fixed paraffin-embedded (FFPE) blocks after a written informed consent was obtained from the research subjects by the Tel Aviv Sourasky Medical Center, under an approved institutional review board (IRB) (0137-21-TLV). Clinical data was obtained from patients' electronic medical records.

Mice tumor xenograft study

Mice maintenance and experiments were carried out under institutional guidelines of the Sourasky Medical Center in accordance with current regulations and standards of the institution Animal Care and Use Committee. We used a subcutaneous mouse model to test the tumorigenic properties and chemoresistance of WT-ER, and D538G-ER –stably expressing cells. Six- week old female athymic nude

mice were purchased from Envigo RMS (Jerusalem, Israel). The mice were housed and maintained in laminar flow cabinets under specific pathogen-free conditions. Estrogen pellets (0.36mg/pellet, 90- days release; Innovative Research of America, Sarasota, Florida, USA; Cat.No. SE-121) were inserted dorsally one week after acclimation. Tumors were induced by injecting 5x106 cells/200µl PBS with Matrigel (1:1 ratio) to mouse flank, 5–6 mice per group. When tumor size reached 100-150mm^3, mice were treated with paclitaxel (Taxol; obtained from the Institution pharmacy) or control PBS intraperitoneally. Paclitaxel was given at a dose of 20mg/kg/week, once a week, for six consecutive weeks. Tumors were measured twice weekly using a caliper by the ellipsoid volume calculation formula 0.5 × (length × width2).

UCSC cancer genomics browser analysis

The heat map and correlation between ABCB1 (MDR1) and c-Jun were constructed by data mining in the Tumor Cancer Genome Atlas (TCGA) breast cancer using the UCSC Xena browser (http://xena.ucsc.edu/).

Statistical analysis

Statistical analysis was performed using the GraphPad Prism software (GraphPad Software): One Way or Two-Way ANOVA with multiple comparisons Bonferroni post hoc analysis and considered significant at P-values * ≤ 0.05, ** ≤ 0.01 and ***≤ 0.001 Bar graphs represent mean and standard deviation (SD) across multiple independent experimental repeats.

Results

LBD mutations associated with decreased sensitivity to chemotherapy

We first aimed to study the sensitivity of BC cells harboring ESR1 activating mutations to doxorubicin and paclitaxel, some of the most commonly used drugs in MBC[25]. Cells expressing mutated ER (mut-ER) showed increased resistance to the drugs (Fig. 1a-b). Thus, paclitaxel at 1nM decreased viability of WT-ER and mut-ER cells by 80% and 50%, respectively (Fig. 1a, $p < 0.001$), and significant differences were observed for all paclitaxel doses. Similarly, none of the WT-ER cells survived 0.5µM doxorubicin, compared to ~ 30% of mutated cells (Fig. 1b, $p < 0.001$). Furthermore, similar results were observed in T47D cells expressing WT-ER, D538G, and Y537S cells. Significant differences were observed for all doxorubicin doses in the mutated cells (Supplementary Fig. 1)

Colony formation assays using 0.5nM paclitaxel and 5nM of doxorubicin (Fig. 1c) yielded similar results. Indeed, mutated cells formed more colonies than WT-ER cells, and the relative decrease in colony number and size was significantly greater in WT-ER cells compared to the mutated cells. Paclitaxel treatment increased colony formation 3- folds in the D538G mutated cells compare to WT-ER and Y537S cells (Fig. 1c, $p < 0.001$). While doxorubicin treatment reduces colony numbers by 90% in WT-ER compared to 70% in both D538G and Y537S cells (Fig. 1c, $p < 0.001$).

LBD-ER mutant cells are resistant to chemotherapy-induced apoptosis

As part of the characterization of chemoresistant cells, we examined the role of apoptosis response in the D538G and Y537S- ER mutant cells. For this aim, cells were treated with chemotherapies for 72 hours and cleaved PARP (c-PARP) levels were monitored. Treatments with paclitaxel and doxorubicin exerted the highest effect on PARP cleavage in WT cells compared to the mut-ER cells (Fig. 2a-b).

In addition, apoptosis studies using Annexin V and 7AAD staining indicated that paclitaxel treatment induced early apoptosis in 12.4% of WT-ER cells compared to 7.1% of D538G and 7.4% of Y537S (Fig. 2c-d).

Mutated ER cells are more resistant to paclitaxel in vivo

In order to study resistance to chemotherapy *in vivo*, female nude mice were first supplemented with estrogen pellet and then injected with D538G or WT-ER MCF-7 cells, (Fig. 3a) and treated with either vehicle control or paclitaxel. While paclitaxel significantly inhibited the tumor growth of the WT-ER group (Fig. 3b, $p < 0.0001$), resistance to paclitaxel was noted in the D538G mice group, and they formed larger tumors compared to WT-ER (Fig. 3b, $p < 0.05$).

Upregulation of the MDR1 in the D538G-ER mutant cells

Overexpression of MDR1 (ABCB1) commonly mediates resistance of cancer cells to paclitaxel and doxorubicin [26]. Therefore, we aimed to study the expression of MDR1 mRNA and the protein it encodes, P-gp, in the mut-ER and WT-ER cells. MDR1 mRNA expression level was 2.3-fold higher in D538G-ER cells ($p < 0.05$, Fig. 4a) and 1.3 in Y537S-ER cells. Accordingly, increased levels of the encoded protein P-gp were noted in the D538G-ER cells compared to both Y537S and WT-ER cells (Fig. 4b-c). In order to corroborate these results, we assessed P-gp levels using IHC in tumor samples derived from an orthotopic mouse model injected with D538G or Y537S ER cells (generated by us previously and described in detail [12]) and noted higher P-gp expression in D538G-ER tumor cells compared to Y537S-ER (Fig. 4d-e). Tumors formed by WT-ER cells were very small and could not be used to assess the P-gp expression. In order to validate this differential effect of the two mutations and eliminate the possibility of clonal effect, expression of the MDR1 gene was also studied in T47D cells expressing either WT-ER, D538G, or Y537S and revealed a similar pattern of MDR1 mRNA and P-gp protein expression (Supplementary Fig. 2a-b).

Next, we aimed to assess the expression profile of P-gp across MBC clinical samples with and without ESR1 mutations. We obtained clinical samples of metastatic breast cancer tumors derived from patients with endocrine resistance, either harboring the ESR1 mutations ($n = 6$), or with WT-ER ($n = 7$).Our results showed a significant elevation in P-gp expression within ESR1 mutation group compared to the control ($p = 0.0311$, Fig. 4f-g and Supplementary Fig. 3). These patients mostly harbor the D538G mutations that metastasize to either bone or liver (Supplementary Table 1). Our results showed increased expression of

P-gp was associated with liver metastasis. To strengthen the association between ESR1 mutations and liver metastasis, we analyzed 1918 tumor samples from a publicly available primary and metastatic breast cancer dataset and focused on 495 metastatic samples obtained from bone, liver, lung, or lymph nodes. We conclude that while WT-ESR1 tumors disseminate in similar proportion between the different sites, ESR1 mutation changes the pattern of metastasis (Supplementary Table 2, P-value = 3.804366x10-05) with liver being 2–3 times more prevalent than the other metastatic sites.

JNK/c-Jun signaling pathway is elevated in the mut-ER cells

MDR1 expression is known to be regulated by the JNK/c-Jun signaling pathway[21,27,28] and this pathway is implicated in conferring chemoresistance[29–31]. First, we studied c-Jun mRNA levels and found 2.8 and 3.4 -fold higher expression in D538G and Y537S -ER cells, respectively (Fig. 5a). Next, we examined the expression of phosphorylated (p)- JNK and c-Jun in mut-ER cells. We found that mut-ER cells, especially D538G cells, expressed higher levels of p-JNK and p-c-Jun compared to WT-ER cells (Fig. 5b-d). In order to eliminate the possibility of clonal effects, we studied the expression of p-JNK and p-c-Jun in additional mut-ER clones and observed a similar higher expression of these proteins in these clones (Supplementary Fig. 4). Furthermore, a similar trend was observed in T47D cells (Supplementary Fig. 5a-b). Next, we aimed to study c-Jun transcriptional activity in the mut-ER compared to that in WT-ER. To this aim, we measured the AP1-luciferase reporter gene and observed a nearly 2-fold increase in AP-1 transcriptional activity in the mut –ER cells ($p < 0.01$, Fig. 5e). In accordance with these results, IHC staining of mice tumor samples that were injected with the mut–ER cells, as previously described [12], showed higher p-JNK expression in D538G tumors compared to Y537S tumors (Fig. 5f-g).

JNK/c-Jun pathway upregulates MDR1 expression, especially in D538G mutant cells

As studies have shown that the JNK/c-Jun signaling pathway induces MDR1 expression [21,27,28], we hypothesized that JNK inhibition would reduce MDR1 expression. To confirm this effect, we inhibited JNK using a commonly used inhibitor, SP600125 (SP). Our results show that its inhibition decreased MDR1 mRNA (Fig. 6a) and protein levels, especially in D538G cells (Fig. 6b). Similar results were produced when treated with an additional JNK inhibitor, BI-78D3 (Supplementary Fig. 6a- b). We confirmed the potency of these inhibitors by monitoring p-c-Jun expression (Supplementary Fig. 7).

Our next aim was to elucidate whether the JNK/c-Jun pathway directly regulates MDR1 expression, thus, we performed a ChIP assay to reveal whether c-Jun directly binds to the MDR1 promoter. We conducted PCR, flanking the AP-1 binding site, in the MDR1 promoter region following c-Jun immunoprecipitation. The results showed a PCR product in D538G and Y537S–ER mutant cells, yet intensity was higher in D538G-ER cells, and no PCR product was observed in the WT-ER cells (Fig. 6c). These results suggest that c-Jun directly transcribes the MDR1 gene in mut-ER cells, mainly in the D538G mutated cells. Collectively, our results showed a more pronounced increase in JNK/c-Jun and MDR1 expressions in D538G mutations in both MCF-7 and T47D cells. These data emphasize that the two mutations differ in their

mechanisms of chemoresistance. Importantly, we verified that ER does not directly induce MDR1 expression. We analyzed 3000bp upstream of the MDR1 promoter, and did not detect classical ER binding sites (conducted using http://gene-regulation.com/pub/programs/alibaba2/).

In order to study the relationship between ABCB1 (MDR1) and JUN expressions in breast cancer clinical samples, we analyzed TCGA transcriptomic databases. Using the UCSC Xena Browser (http://xena.ucsc.edu/), we found a positive correlation between JUN and ABCB1 ($r = 0.3782$, $p = 1.038e-42$ based on Pearson's correlation and $r = 0.3782$, $p = 1.038e-42$ based on Spearman's correlation) (Fig. 6d).

JNK inhibition sensitizes breast cancer cells to chemotherapy

We aimed to reveal whether modulation of the JNK signaling pathway can restore sensitivity to chemotherapy in the mut-ER cells. First, we studied the effect of JNK inhibition on apoptosis in the mut-ER and WT-ER cells. We treated cells with the JNK inhibitor SP, examined c-PARP expression, and found that JNK inhibition induced apoptosis, mostly in D538G cells (Fig. 7a). In order to determine the role of JNK in mediating chemoresistance in these cells, we compared cell viability after treatment with doxorubicin, SP, or their combination. As expected, the results showed that mut-ER cells were more resistant to doxorubicin treatment ($p < 0.001$ compared to WT-ER). Interestingly, while SP inhibited both WT-ER and mut-ER cells, WT-ER cells were more affected (45% vs 55% viability). Importantly, co-treatment with SP and doxorubicin sensitized mut-ER cells to doxorubicin. Of note, co-treatment of WT-ER cells did not reduce cells viability beyond doxorubicin alone, which may be due to the strong effect of doxorubicin as a single treatment (Fig. 7b; $p < 0.001$ of D538G cells when treated with combination compared to doxorubicin alone).

Doxorubicin accumulation is decreased in D538G mutated cells

It has been well established that doxorubicin is one of the P-gp substrates and that [32] P-gp diminishes the internalization and accumulation of doxorubicin in cancer cells, leading to chemoresistance[33]. As we showed that D538G mutated cells express higher P-gp levels compared to WT-ER, we first aimed to show that doxorubicin accumulation is reduced in D538G mutated cells. To this aim, we monitored cellular accumulation of fluorescently-label doxorubicin (DOX-F). We treated WT-ER and D538G cells with DOX-F and in accordance with our hypothesis, we observed the fluorescent signal in the nuclei of the D538G mutated cells was lower compared to WT-ER cells (Fig. 8a-b). In order to validate that the JNK pathway modulates P-gp expression and hence activity, cells were treated with DOX-F and SP together. Indeed, the intensity of DOX-F fluorescence increased upon the addition of SP in the D538G mutated cells (Fig. 8b), suggesting that the JNK pathway regulates doxorubicin intracellular accumulation.

We studied intracellular accumulation of doxorubicin also using FACS analysis. In agreement with the imaging data, doxorubicin accumulated more in D538G-ER cells compared to WT-ER cells (Fig. 8d, $p < 0.01$). Furthermore, SP treatment increased fluorescence intensity only in D538G cells (Fig. 8c-d; $p < 0.05$). These results strongly suggest a decrease in doxorubicin accumulation in the D538G cells as they are resistant to chemotherapy. In addition, there is a strong link between the activation of the JNK pathway and increase intracellular retention of doxorubicin.

Discussion

Approximately 40% of patients with ER-positive metastatic breast cancer acquire resistance to endocrine therapy due to the acquisition of LBD-ER mutations[34]. Importantly, this group of patients often have a more aggressive disease and worse prognosis[35]. Chemoresistance continues to be a major obstacle that impairs the efficacy of cancer therapy and nearly 90% of patients fail to respond to chemotherapy due to resistance of cancer cells, either de novo or acquired resistance[36]. As most patients with endocrine resistance are treated with chemotherapy, we hypothesized that reduced response to chemotherapy may contribute to the worse prognosis seen in patients harboring these mutations. Yet, no studies have assessed chemotherapy resistance in ER-positive patients harboring LBD-ER mutations in *in vitro* studies or in *in vivo* models. In our current study, we examined whether LBD-ER mutations confer resistance to chemotherapeutic drugs, specifically to doxorubicin and paclitaxel, which are among the most commonly used chemotherapy drugs for metastatic breast cancer. We discovered that LBD-ER cells are more resistant to chemotherapy compared to the WT-ER cells as using both in vitro and *in vivo* models.

In order to study chemoresistance, we employed the well-established MCF-7 cell model that expresses WT, D538G or Y537S –ER, at physiological levels[12]. Using these cells, we explored the effect of the mutations on viability, colony formation, and apoptosis following treatments with the chemotherapy drugs described above. Our results show that LBD-ER cells are more resistant to chemotherapy compared to the WT-ER cells. Of note, to further investigate chemoresistance, we established an *in vivo* model, and observed that paclitaxel treatment had no effect on tumor growth in mut-ER group, while this treatment led to tumor shrinkage in the WT-ER group (Fig. 3b). It is important to point that while the *in vivo* experiment showed a clear resistance of D538G-ER tumors compared to WT-ER tumors, some factors may have contributed to this behavior. First, we employed subcutaneous implantation approach; thus, drug response may be modulated by different microenvironmental stimuli. Second, we used paclitaxel doses suitable for mice tolerance, and perhaps WT-ER cells would respond to higher doses. Yet, the accumulating data we present strongly suggest a relative resistance to chemotherapy in mut-ER cells. Patients with endocrine-resistant MBC often receive CDK and PI3K inhibitors as part of their treatment regimen[37]. Interestingly, the impact of ESR1 mutations on the response to these inhibitors is still debatable, with some studies indicating that these mutations do not predict treatment response, while others have demonstrated a reduced response associated with ESR1 mutations[38]. These findings emphasize the necessity for developing novel drugs that can enhance treatment response and potentially prolong survival in patients with ESR1 mutations.

There are several mechanisms that enable BC cells to acquire drug resistance. Among these are the well characterized P-gp transporters, which are encoded by the MDR1 gene[39]. Doxorubicin is one of the major substrates of P-gp, therefore it plays a role in the internalization of doxorubicin[40]. Similarly, low doxorubicin accumulation has been reported in MDR cell lines including MCF-7^{ADR}[41]. Indeed, we have shown that doxorubicin accumulation was lower in the D538G mutated cells compared to WT-ER (Fig. 8b). We also evaluated this gene expression on the mRNA and protein levels, and found that MDR1 protein expression is elevated in LBD-ER mutant cells, though more prominently in D538G, compared to the WT-ER (Fig. 4a-c). In agreement with these results, we found an increase in the P-gp expression level in patients' samples harboring the ESR1 mutations compared to patients without the mutation (Fig. 4f,g). Our results suggest that the mut-ER cells are able to utilize the P-gp transporters as part of their resistance mechanism to overcome chemotherapy treatments. A relationship between endocrine treatment and P-gp was demonstrated previously, showing that tamoxifen increases sensitivity to doxorubicin, and increases accumulation of vinblastine in MCF7 cells expressing MDR1[42]. On the other hand, another study showed that WW domain-binding protein 2 (WBP2) can bind ER, leading increased MDR1 expression[43].

We aimed to reveal the mechanism through which mut-ER induces MDR1 expression. Although MDR1 expression was observed primarily in mut-ER cells, we first confirmed that there are no ER binding sites on the MDR1 promoter. In search for a possible mechanism, we focused on the JNK/c-Jun pathway as it has been shown to play a role in chemoresistance of some types of cancer[44–46]. Thus, activation of JNKs that resulted in transcriptional activity of c-Jun, also led to the transcription of other genes related to drug resistance, like XIAP, c-fos and JunB[47,48]. Therefore, our goal was to reveal whether the JNK pathway was differentially regulated in LBD-ER cells. We observed activation of the JNK/c-Jun pathway as evidenced by high expressions of p-JNK, p-c-Jun and elevated AP-1 transcriptional activity in the LBD-ER mutant cells compared to WT-ER (Fig. 5). These data suggest a role of the JNK pathway in the LBD-ER mutations. Our results are supported by several studies. Increased JNK signaling was observed following long term acquisition of resistance to endocrine therapies[49]. Another study showed that activation of the JNK pathway is associated with everolimus resistance in endocrine resistant cells[50]. Noteworthy, the important role AP-1 plays in endocrine resistance was demonstrated in a study where inhibition of AP-1, in both in vitro and *in vivo* settings, enhanced anti proliferative effect of endocrine treatments and delayed the onset of tamoxifen resistance in mice model[51].

The JNK/c-Jun pathway is known to be associated with MDR1 expression. Several studies have shown that JNK/c-Jun pathway is activated in cancer cells that acquired resistance to chemotherapy in vitro, demonstrating the importance in regulating MDR1 expression[21,23,28]. To test this, we first showed that SP600125, an inhibitor of the JNK signaling pathway, downregulated the expression of P-gp and MDR1, especially in the D538G cells. To provide additional evidence, we performed a ChIP assay and indeed our results showed an increase in c-Jun occupancy in the MDR1 promoter, leading to an increase in P-gp transporters in the mutated cells. In addition, a bioinformatics analysis of TCGA breast cancer BRCA

database showed a strong positive correlation between JUN and ABCB1, confirming our results that c-Jun potentiates the MDR1 expression in BC cells.

The JNK/c-Jun pathway emerged as a differentially activated pathway in mut-ER cells that directly regulates MDR1 expression. Hence, our next aim was to assess whether this pathway may serve as a novel target for mut-ER breast cancer tumors. We studied viability and apoptosis of WT and mut –ER cells treated with JNK inhibitors and found that JNK inhibition decreased viability in both WT and D538G cells but significantly increased apoptosis in the D538G mutated cells. Previously, it was shown that JNK inhibition decreased cell growth in nasopharyngeal carcinoma[52] and triple- negative breast cancer[53]. As we found that c-Jun directly induces MDR1 expression, we aimed to reveal whether inhibition of c-Jun activity would restore cell sensitivity to chemotherapy. Indeed, using a JNK inhibitor (SP600125) we were able to sensitize cells to doxorubicin. This effect was observed in all cell lines, with highest effect in D538G-ER cells. Indeed, it was shown that SP600125 reduced viability of breast cancer cells which acquired resistance to doxorubicin [54]. In addition, a different study, in nasopharyngeal carcinoma cancer cells, showed that doxorubicin treatment combined with SP600125 more effectively inhibited cell growth than the single treatments[52]. Indeed, we showed that JNK inhibition led to increase the accumulation of doxorubicin in the D538G-ER cells. These results imply that doxorubicin resistance can be accounted for by decreased amounts of drug at nuclear targets, which may be mediated by the expression and function of P-gp.

Interestingly, while Y537S and D538G exhibit similar behavior, a detailed analysis suggests some subtle, yet potentially important differences. Thus, we observed less JNK phosphorylation in Y537S cells compared to D538G cells (as verified by analyzing different stable clones, supplementary Fig. 3). Additionally, we noted higher MDR1 expression in D538G cells and lower binding of c-Jun to MDR1 promoter in Y537S cells (Fig. 6c). These results suggest unique characteristics for each mutation despite their similar role in conferring endocrine resistance. Consistent with our observations, previous studies have also revealed notable differences between Y537S and D538G. For example, Y537S confers higher endocrine resistance than D538G cells and is associated with a shorter overall survival[55].

While we focused on the JNK-MDR1 axis in mut-ER cells, studies showed that resistance to chemotherapy in breast cancer could evolve from a wide array of mechanisms[56], some of them are relevant to mut-ER cells. For example, active PI3K/mTOR pathway may lead to resistance to chemotherapy[57], and several studies including ours[12,58] showed increased activation of this pathway in mut-ER cells.

Taken together, our current study demonstrates that activating mutations in the LBD-ER not only confer resistance to endocrine therapy but also relative resistance to commonly used chemotherapy. This resistance is, at least in part, mediated by the activation of the JNK/c-Jun pathway, leading to the upregulation of MDR1 expression (Fig. 8e). These findings underscore the urgency of discovering new drugs to effectively treat patients with ESR1-mutated tumors, as these tumors display decreased responsiveness even to subsequent lines of treatment such as chemotherapy. Moreover, the study

highlights the significance of targeting the JNK/c-Jun as a strategy to sensitize mut-ER cells to chemotherapy. Furthermore, this study reveals distinct differences between the Y537S and D538G mutations, emphasizing the importance of carefully examining these discrepancies, as they may hold implications for the treatment of patients harboring these specific mutations.

Abbreviations

BC
Breast cancer
MBC
Metastatic breast cancer
ERα
Estrogen receptor-a
LBD
Ligand binding domain
MDR1
Multiple drug resistance-1
P-gp
P-glycoprotein
JNK
c-Jun N-terminal kinase

Declarations

The authors declare no potential conflicts of interest.

Authors' contributions- MT- Collected the data, performed the analysis of in vitro and in vivo assays, and wrote the manuscript. AZ- contributed in data analysis. ZH- performed analysis on patients' data and contributed in analysis. AK- contributed in data analysis. OM- Contributed data and analysis tools, performed analysis on patient's data. IW- Conceived and designed the analysis, collected the data, performed analysis, and wrote the paper. TR- Conceived and designed the analysis, collected the data, performed analysis, and wrote the paper. All authors read and approved the final manuscript.

Ethical Approval- All procedures performed in studies involving human clinical samples were in accordance with a written informed consent obtained from the research subjects by the Tel Aviv Sourasky Medical Center, under an approved institutional review board (IRB) (0137-21-TLV). The experiments on animals were conducted in accordance with institutional guidelines of the Sourasky Medical Center in accordance with current regulations and standards of the institution Animal Care and Use Committee.

Funding- Not applicable

Availability of data and materials- The datasets used and/or analyzed during the current study are available from the corresponding author on reasonable request.

References

1. Torre LA, Bray F, Siegel RL, Ferlay J, Lortet-Tieulent J, Jemal A. Global cancer statistics, 2012. CA Cancer J Clin. 2015. doi:10.3322/caac.21262
2. Merenbakh-Lamin K, Ben-Baruch N, Yeheskel A, et al. D538G mutation in estrogen receptor-α: A novel mechanism for acquired endocrine resistance in breast cancer. Cancer Res. 2013;73(23):6856–6864. doi:10.1158/0008-5472.CAN-13-1197
3. Robinson DR, Wu YM, Vats P, et al. Activating ESR1 mutations in hormone-resistant metastatic breast cancer. Nat Genet. 2013. doi:10.1038/ng.2823
4. Toy W, Shen Y, Won H, et al. ESR1 ligand-binding domain mutations in hormone-resistant breast cancer. Nat Genet. 2013. doi:10.1038/ng.2822
5. Li S, Shen D, Shao J, et al. Endocrine-Therapy-Resistant ESR1 Variants Revealed by Genomic Characterization of Breast-Cancer-Derived Xenografts. Cell Rep. 2013. doi:10.1016/j.celrep.2013.08.022
6. Jeselsohn R, Yelensky R, Buchwalter G, et al. Emergence of constitutively active estrogen receptor-α mutations in pretreated advanced estrogen receptor-positive breast cancer. Clin Cancer Res. 2014. doi:10.1158/1078-0432.CCR-13-2332
7. Fribbens C, O'Leary B, Kilburn L, et al. Plasma ESR1 Mutations and the treatment of estrogen receptor-Positive advanced breast cancer. J Clin Oncol. 2016. doi:10.1200/JCO.2016.67.3061
8. Schiavon G, Hrebien S, Garcia-Murillas I, et al. Analysis of ESR1 mutation in circulating tumor DNA demonstrates evolution during therapy for metastatic breast cancer. Sci Transl Med. 2015. doi:10.1126/scitranslmed.aac7551
9. Jeselsohn R, De Angelis C, Brown M, Schiff R. The Evolving Role of the Estrogen Receptor Mutations in Endocrine Therapy-Resistant Breast Cancer. Curr Oncol Reports 2017 195. 2017;19(5):1–8. doi:10.1007/S11912-017-0591-8
10. Gyanchandani R, Kota KJ, Jonnalagadda AR, et al. Detection of ESR1 mutations in circulating cell-free DNA from patients with metastatic breast cancer treated with palbociclib and letrozole. Oncotarget. 2017. doi:10.18632/oncotarget.11383
11. Jeselsohn R, Buchwalter G, De Angelis C, Brown M, Schiff R. ESR1 mutations-a mechanism for acquired endocrine resistance in breast cancer. Nat Rev Clin Oncol. 2015. doi:10.1038/nrclinonc.2015.117
12. Zinger L, Merenbakh-Lamin K, Klein A, et al. Ligand-binding Domain–activating Mutations of ESR1 Rewire Cellular Metabolism of Breast Cancer Cells. Clin Cancer Res. 2019. doi:10.1158/1078-0432.ccr-18-1505

13. Chandarlapaty S, Chen D, He W, et al. Prevalence of ESR1 Mutations in Cell-Free DNA and Outcomes in Metastatic Breast Cancer: A Secondary Analysis of the BOLERO-2 Clinical Trial. JAMA Oncol. 2016. doi:10.1001/jamaoncol.2016.1279
14. Longley DB, Johnston PG. Molecular mechanisms of drug resistance. J Pathol. 2005. doi:10.1002/path.1706
15. Zahreddine H, Borden KLB. Mechanisms and insights into drug resistance in cancer. Front Pharmacol. 2013. doi:10.3389/fphar.2013.00028
16. Xia Y, Yang W, Bu W, et al. Reversal of P-glycoprotein-mediated multidrug resistance in cancer cells by the c-Jun NH2-terminal kinase. Mol Cancer Ther. 2013. doi:10.1158/1535-7163.MCT-14-0011
17. Linardi RL, Natalini CC. Multi-drug resistance (MDR1) gene and P-glycoprotein influence on pharmacokinetic and pharmacodymanic of therapeutic drugs. Ciência Rural. 2006. doi:10.1590/s0103-84782006000100056
18. Januchowski R, Sterzyńska K, Zaorska K, et al. Analysis of MDR genes expression and cross-resistance in eight drug resistant ovarian cancer cell lines. J Ovarian Res. 2016. doi:10.1186/s13048-016-0278-z
19. Fung TS, Liu DX. Activation of the c-Jun NH2-terminal kinase pathway by coronavirus infectious bronchitis virus promotes apoptosis independently of c-Jun article. Cell Death Dis. 2017. doi:10.1038/s41419-017-0053-0
20. Zhu MM, Tong JL, Xu Q, et al. Increased JNK1 signaling pathway is responsible for ABCG2-mediated multidrug resistance in human colon cancer. PLoS One. 2012. doi:10.1371/journal.pone.0041763
21. Wang PP, Luan JJ, Xu WK, et al. Astragaloside IV downregulates the expression of MDR1 in Bel-7402/FU human hepatic cancer cells by inhibiting the JNK/c-Jun/AP-1 signaling pathway. Mol Med Rep. 2017. doi:10.3892/mmr.2017.6924
22. Zhou J, Liu M, Aneja R, Chandra R, Lage H, Joshi HC. Reversal of P-glycoprotein-mediated multidrug resistance in cancer cells by the c-Jun NH2-terminal kinase. Cancer Res. 2006. doi:10.1158/0008-5472.CAN-05-1779
23. Priyamvada S, Anbazhagan AN, Kumar A, et al. Lactobacillus acidophilus stimulates intestinal P-glycoprotein expression via a c-Fos/c-Jun-dependent mechanism in intestinal epithelial cells. Am J Physiol - Gastrointest Liver Physiol. 2016;310(8):G599. doi:10.1152/AJPGI.00210.2015
24. Kaemmerer D, Peter L, Lupp A, et al. Comparing of IRS and Her2 as immunohistochemical scoring schemes in gastroenteropancreatic neuroendocrine tumors. Int J Clin Exp Pathol. 2012;5(3):187. /pmc/articles/PMC3341681/. Accessed March 25, 2023.
25. Hanna, PharmD, BCPS, BCOP K, Mayden, MSN, FNP, AOCNP K. Chemotherapy Treatment Considerations in Metastatic Breast Cancer. J Adv Pract Oncol. 2021;12(Suppl 2):6. doi:10.6004/JADPRO.2021.12.2.11
26. Vaidyanathan A, Sawers L, Gannon AL, et al. ABCB1 (MDR1) induction defines a common resistance mechanism in paclitaxel- and olaparib-resistant ovarian cancer cells. Br J Cancer. 2016. doi:10.1038/bjc.2016.203

27. Chen Q, Bian Y, Zeng S. Involvement of AP-1 and NF-κB in the Up-regulation of P-gp in Vinblastine Resistant Caco-2 Cells. Drug Metab Pharmacokinet. 2013. doi:10.2133/dmpk.dmpk-13-sh-068
28. Daschner PJ, Ciolino HP, Plouzek CA, Yeh GC. Increased AP-1 activity in drug resistant human breast cancer MCF-7 cells. Breast Cancer Res Treat. 1999. doi:10.1023/A:1006138803392
29. Dou Y, Jiang X, Xie H, He J, Xiao S. The Jun N-terminal kinases signaling pathway plays a “seesaw” role in ovarian carcinoma: A molecular aspect. J Ovarian Res. 2019. doi:10.1186/s13048-019-0573-6
30. Yan D, An GY, Kuo MT. C-Jun N-terminal kinase signalling pathway in response to cisplatin. J Cell Mol Med. 2016. doi:10.1111/jcmm.12908
31. Lipner MB, Peng XL, Jin C, et al. Irreversible JNK1-JUN inhibition by JNK-IN-8 sensitizes pancreatic cancer to 5-FU/FOLFOX chemotherapy. JCI Insight. 2020. doi:10.1172/jci.insight.129905
32. Jianmongkol S. Overcoming P-Glycoprotein-Mediated Doxorubicin Resistance. In: Advances in Precision Medicine Oncology.; 2021. doi:10.5772/intechopen.95553
33. Waghray D, Zhang Q. Inhibit or Evade Multidrug Resistance P-Glycoprotein in Cancer Treatment. J Med Chem. 2018. doi:10.1021/acs.jmedchem.7b01457
34. Angus L, Beije N, Jager A, Martens JWM, Sleijfer S. ESR1 mutations: Moving towards guiding treatment decision-making in metastatic breast cancer patients. Cancer Treat Rev. 2017. doi:10.1016/j.ctrv.2016.11.001
35. Reinert T, Saad ED, Barrios CH, Bines J. Clinical Implications of ESR1 Mutations in Hormone Receptor-Positive Advanced Breast Cancer. Front Oncol. 2017. doi:10.3389/fonc.2017.00026
36. Wang Y, Wan G-H, Wu Y-M, et al. AP-1 confers resistance to anti-cancer therapy by activating XIAP. Oncotarget. 2018. doi:10.18632/oncotarget.23897
37. Cardoso F, Paluch-Shimon S, Senkus E, et al. 5th ESO-ESMO international consensus guidelines for advanced breast cancer (ABC 5). Ann Oncol. 2020. doi:10.1016/j.annonc.2020.09.010
38. Brett JO, Spring LM, Bardia A, Wander SA. ESR1 mutation as an emerging clinical biomarker in metastatic hormone receptor-positive breast cancer. Breast Cancer Res. 2021;23(1). doi:10.1186/S13058-021-01462-3
39. Chen KG, Sikic BI. Molecular pathways: Regulation and therapeutic implications of multidrug resistance. Clin Cancer Res. 2012;18(7):1863–1869. doi:10.1158/1078-0432.CCR-11-1590/84701/AM/MOLECULAR-PATHWAYS-REGULATION-AND-THERAPEUTIC
40. Kibria G, Hatakeyama H, Akiyama K, Hida K, Harashima H. Comparative study of the sensitivities of cancer cells to doxorubicin, and relationships between the effect of the drug-efflux pump P-gp. Biol Pharm Bull. 2014. doi:10.1248/bpb.b14-00529
41. Schuurhuis GJ, Van Heijningen THM, Cervantes A, et al. Changes in subcellular doxorubicin distribution and cellular accumulation alone can largely account for doxorubicin resistance in SW-1573 lung cancer and MCF-7 breast cancer multidrug resistant tumour cells. Br J Cancer. 1993. doi:10.1038/bjc.1993.452

42. Effect of Tamoxifen on the Multidrug-resistant Phenotype in Human Breast Cancer Cells: Isobologram, Drug Accumulation, and Mr 170,000 Glycoprotein (gp170) Binding Studies1 | Cancer Research | American Association for Cancer Research. https://aacrjournals.org/cancerres/article/54/2/441/500670/Effect-of-Tamoxifen-on-the-Multidrug-resistant. Accessed June 19, 2023.
43. Chen S, Wang H, Li Z, et al. Interaction of WBP2 with ERα increases doxorubicin resistance of breast cancer cells by modulating MDR1 transcription. Br J Cancer. 2018;119(2):182–192. doi:10.1038/S41416-018-0119-5
44. Hu L, Zou F, Grandis JR, Johnson DE. The JNK Pathway in Drug Resistance. In: Targeting Cell Survival Pathways to Enhance Response to Chemotherapy.; 2018. doi:10.1016/b978-0-12-813753-6.00004-4
45. Suzuki S, Okada M, Shibuya K, et al. JNK suppression of chemotherapeutic agents-induced ROS confers chemoresistance on pancreatic cancer stem cells. Oncotarget. 2015;6(1):458. doi:10.18632/ONCOTARGET.2693
46. Yan D, An GY, Kuo MT. C-Jun N-terminal kinase signalling pathway in response to cisplatin. J Cell Mol Med. 2016;20(11):2013–2019. doi:10.1111/JCMM.12908
47. Papachristou DJ, Batistatou A, Sykiotis GP, Varakis I, Papavassiliou AG. Activation of the JNK-AP-1 signal transduction pathway is associated with pathogenesis and progression of human osteosarcomas. Bone. 2003. doi:10.1016/S8756-3282(03)00026-7
48. Wang Y, Wan GH, Wu YM, et al. AP-1 confers resistance to anti-cancer therapy by activating XIAP. Oncotarget. 2018. doi:10.18632/oncotarget.23897
49. Piggott L, Silva A, Robinson T, et al. Acquired resistance of er-positive breast cancer to endocrine treatment confers an adaptive sensitivity to trail through posttranslational downregulation of c-FLIP. Clin Cancer Res. 2018. doi:10.1158/1078-0432.CCR-17-1381
50. Kimura M, Hanamura T, Tsuboi K, et al. Acquired resistance to everolimus in aromatase inhibitorresistant breast cancer. Oncotarget. 2018. doi:10.18632/oncotarget.25133
51. Malorni L, Giuliano M, Migliaccio I, et al. Blockade of AP-1 potentiates endocrine therapy and overcomes resistance. Mol Cancer Res. 2016. doi:10.1158/1541-7786.MCR-15-0423
52. Liu Y, Feng J, Zhao M, et al. JNK pathway inhibition enhances chemotherapeutic sensitivity to adriamycin in nasopharyngeal carcinoma cells. Oncol Lett. 2017. doi:10.3892/ol.2017.6349
53. Soleimani M, Somma A, Kaoud T, et al. Covalent JNK Inhibitor, JNK-IN-8, Suppresses Tumor Growth in Triple-Negative Breast Cancer by Activating TFEB- and TFE3-Mediated Lysosome Biogenesis and Autophagy. Mol Cancer Ther. 2022;21(10):1547–1560. doi:10.1158/1535-7163.MCT-21-1044/707989/AM/COVALENT-JNK-INHIBITOR-JNK-IN-8-SUPPRESSES-TUMOR
54. Kim JH, Kim TH, Kang HS, Ro J, Kim HS, Yoon S. SP600125, an inhibitor of Jnk pathway, reduces viability of relatively resistant cancer cells to doxorubicin. Biochem Biophys Res Commun. 2009. doi:10.1016/j.bbrc.2009.07.036

55. Bahreini A, Li Z, Wang P, et al. Mutation site and context dependent effects of ESR1 mutation in genome-edited breast cancer cell models. Breast Cancer Res. 2017. doi:10.1186/s13058-017-0851-4
56. Lainetti P de F, Leis-Filho AF, Laufer-Amorim R, Battazza A, Fonseca-Alves CE. Mechanisms of Resistance to Chemotherapy in Breast Cancer and Possible Targets in Drug Delivery Systems. Pharmaceutics. 2020;12(12):1–20. doi:10.3390/PHARMACEUTICS12121193
57. Gremke N, Polo P, Dort A, et al. mTOR-mediated cancer drug resistance suppresses autophagy and generates a druggable metabolic vulnerability. Nat Commun. 2020;11(1). doi:10.1038/S41467-020-18504-7
58. Shackleford MT, Rao DM, Bordeaux EK, et al. Estrogen Regulation of mTOR Signaling and Mitochondrial Function in Invasive Lobular Carcinoma Cell Lines Requires WNT4. Cancers (Basel). 2020;12(10):1–22. doi:10.3390/CANCERS12102931

Figures

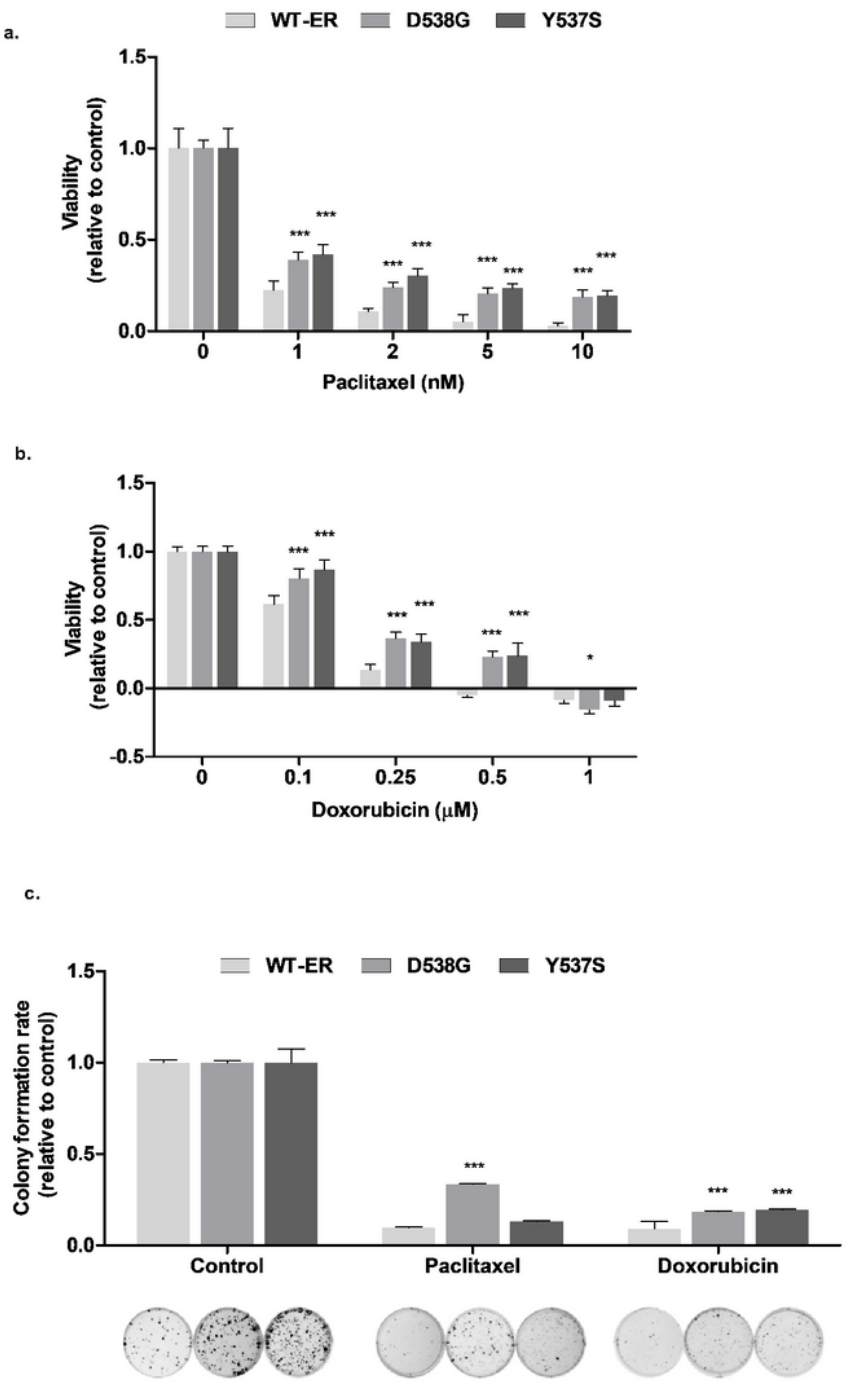

Figure 1

Decreased sensitivity to chemotherapy treatments in the LBD-ER mutant cells.

(a-c) WT-ER and LBD-ER MCF-7 cells were seeded in 96 well plates and treated with indicated concentrations of paclitaxel and doxorubicin for 72 hours. Viability was assessed using methylene blue assay. (d) Cells were seeded at low density and then treated with chemotherapy drugs twice a week for

two weeks, then cells were fixed and colonies stained with crystal violet. Quantification of colonies was done by dissolving in 10% acetic acid and read in a plate reader at 560nm wavelength.

*P<0.05, **P<0.01, ***P<0.001. Each bar represents the mean ± S.D. Experiment was repeated 3 times and a representative experiment is depicted.

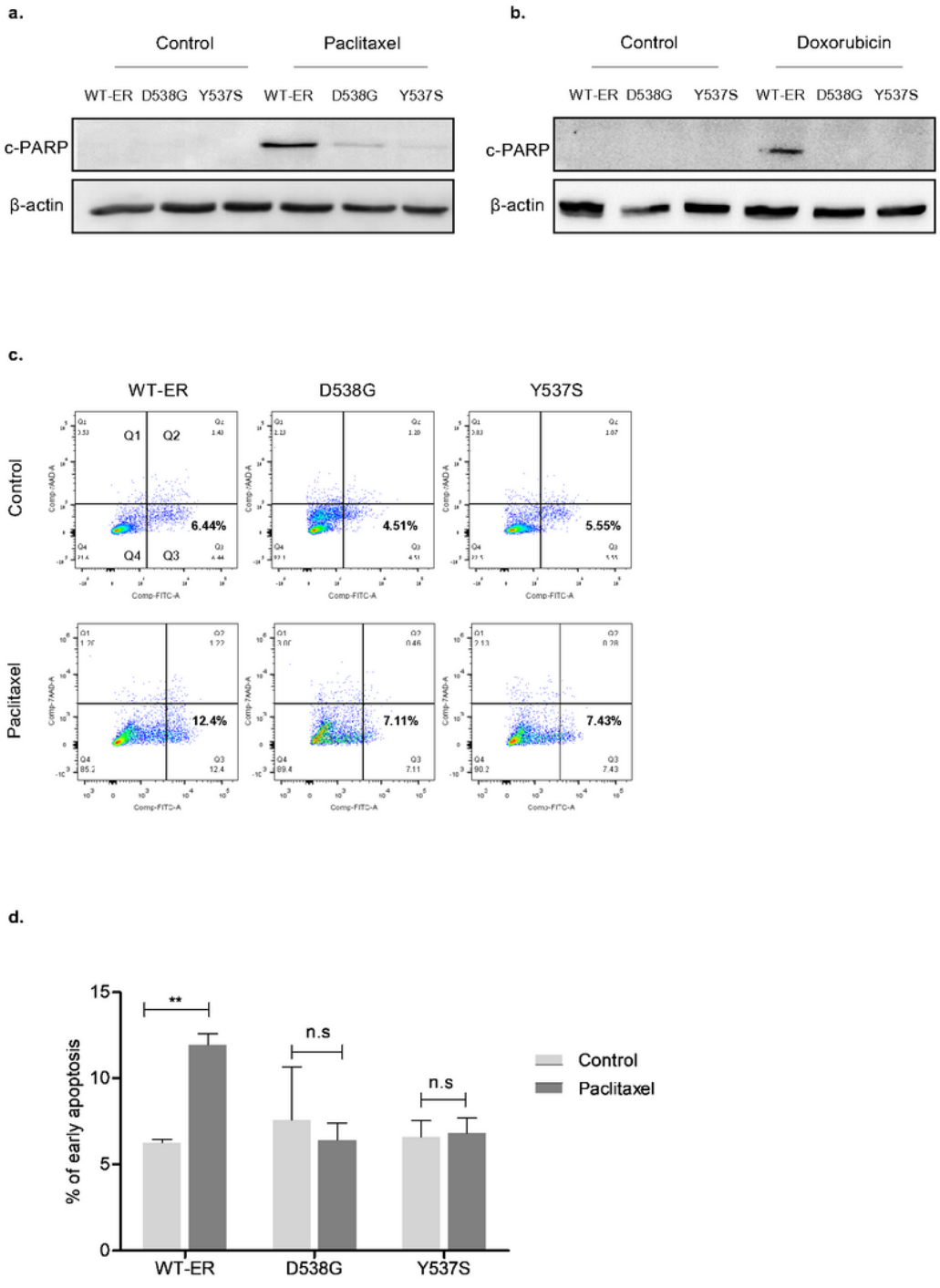

Figure 2

LBD-ER mutant cells exert less apoptosis in response to chemotherapy treatment.

(a-b) WT-ER and LBD-ER MCF-7 cells were treated with 20nM paclitaxel or 200nM doxorubicin for 72 hours. Cells were lysed and immunoblotted with c-PARP. β-actin served as a control. (c) Cells were treated with 20nM paclitaxel for 72 hours then stained with Annexin /7AAD according to the manufacturer's protocol and analyzed by flow cytometry. Representative bar chart demonstrated the number of early apoptotic cells are shown in (d). Figure show representative results of three independent experiments.

*P<0.05, **P<0.01. Each bar represents the mean ± S.D.

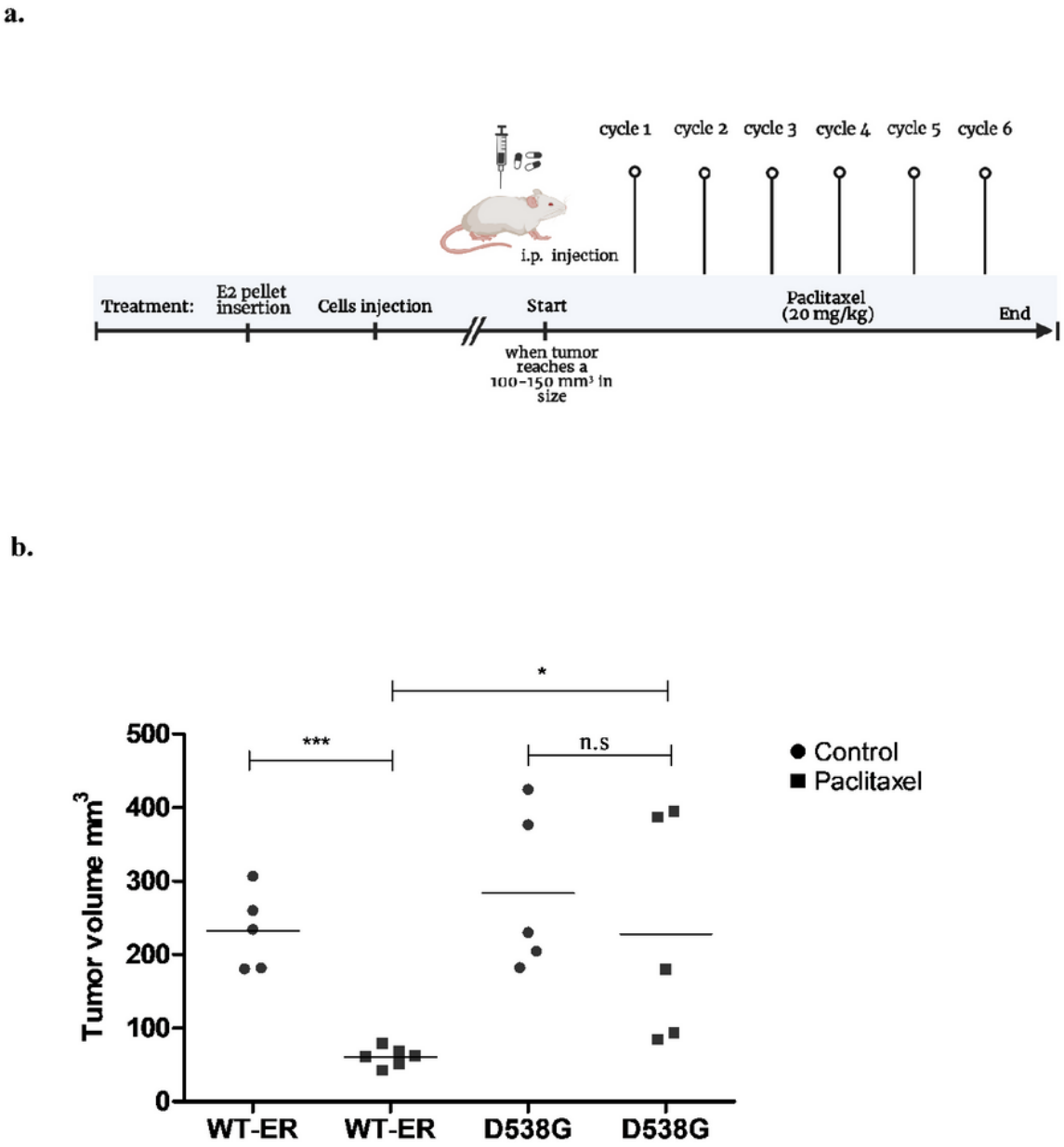

Figure 3

D538G tumors are resistant to paclitaxel in vivo.

(a) Experimental design of paclitaxel treatment *in vivo*. (b) Nude mice were inoculated subcutaneously with WT (n=11) and D538G-ER cells (n=10). When tumor reached 100-150mm^3 in volume, mice were

divided randomly into groups and paclitaxel was administered for 6 weeks. Tumor size was measured twice weekly (*P<0.05; ***P<0.001).

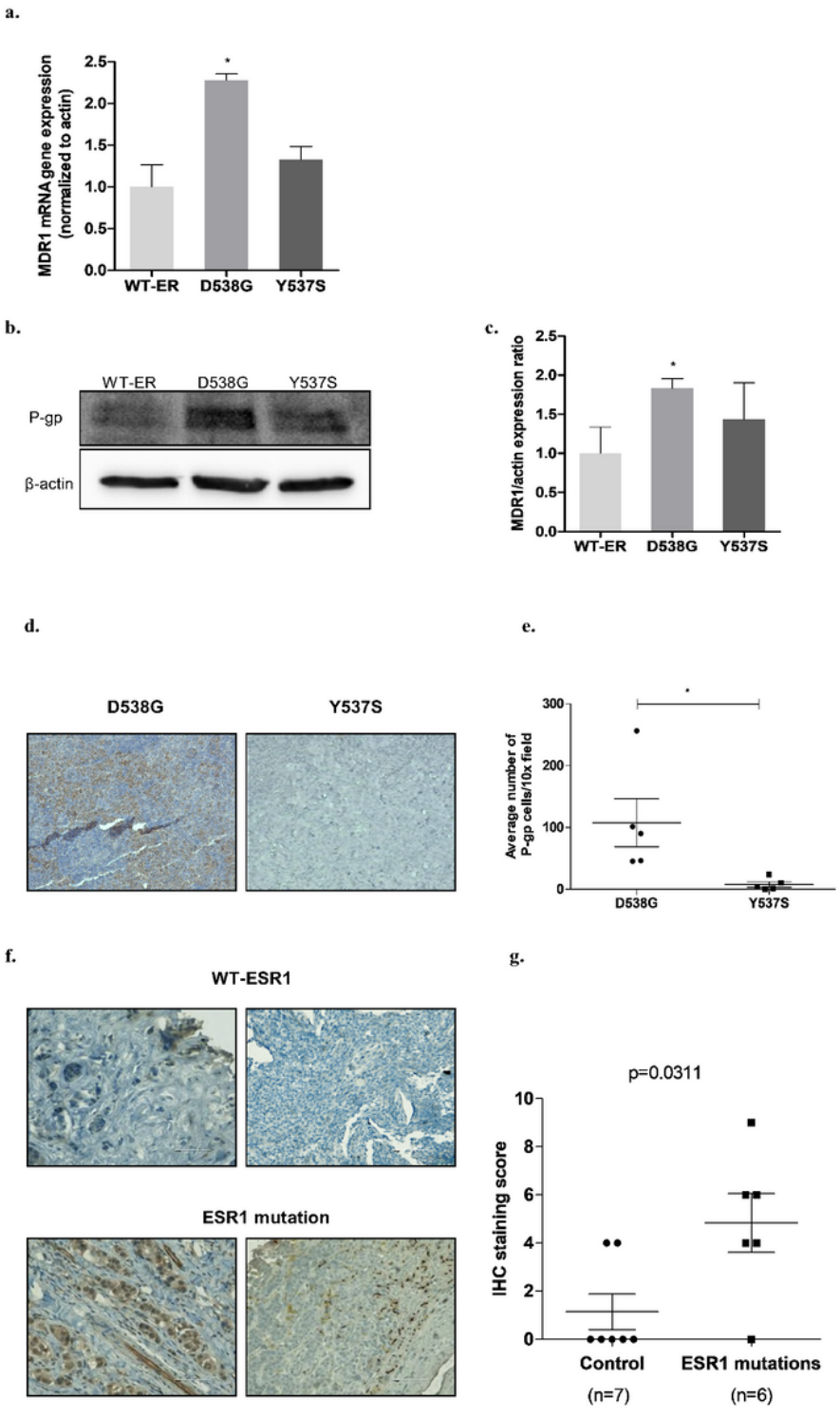

Figure 4

Increased MDR1 expression in the D538G mutated cells.

(a) MDR1 mRNA expression level in the WT-ER and the LBD-ER cells was determined by q-RT-PCR. Values were normalized to β-actin. (b) P-gp protein level was evaluated using western blot. β-actin was used as a loading control. (c) quantification of the MDR1 levels are shown in the histograms (d) IHC staining of P-gp expression in mice tumor samples, D538G (n=5) and Y537S (n=5). Representative photomicrographs (taken with a 10x objective). (e) P-gp relative levels were determined by taking the average of 4 fields per group using Image J. (f) Representative IHC staining of P-gp protein levels in BC metastasis with ESR1 mutations (n=6) and WT-ESR1 (n=7) (g) dot-plot of IHC data quantification (mean ± s.d., unpaired *t*-test). Scale bars represent 80μm. *P<0.05

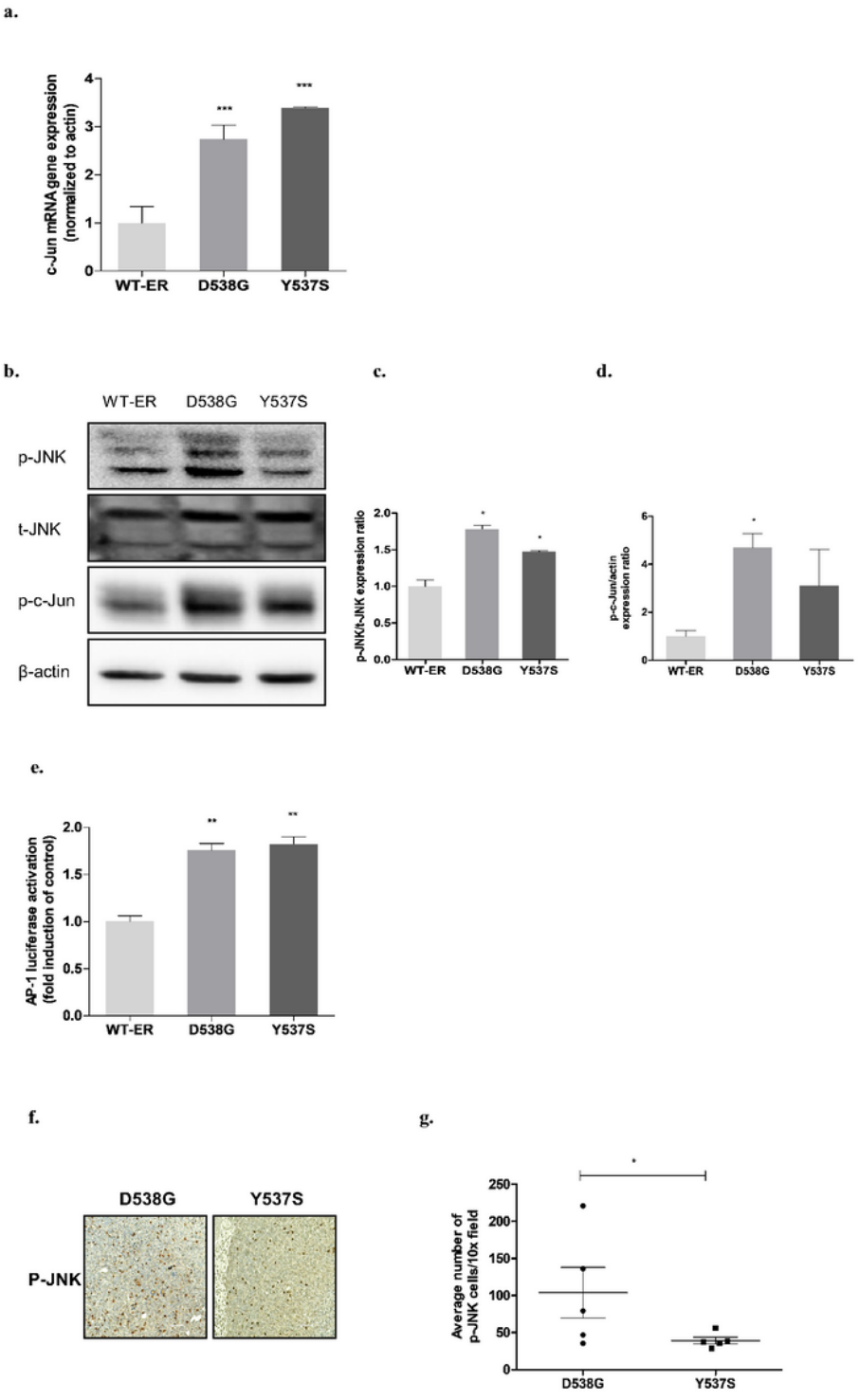

Figure 5

JNK pathway is activated in the mut-ER cells.

(a) c-Jun mRNA expression level in the WT-ER and the LBD-ER cells was determined by q-RT-PCR. Values were normalized to β-actin. (b) p-JNK (T183/Y185), T-JNK, and p-c-Jun (ser73) protein levels were evaluated using western blot. β-actin was used as a loading control. (c,d) quantification of the p-JNK and

p-c-Jun levels are shown in the histograms. (e) Cells were transfected with AP-1-luciferase reporter plasmid. After 24 hours, luciferase assay was performed, and results were normalized to protein concentration. (f) IHC analysis of p-JNK expression in mice tumor samples (D538G (n=5) and Y537S (n=5)) using DAB staining. Representative photomicrographs (taken with a 10x objective). (g) p-JNK relative levels were quantified by taking the average of 4 fields per group using Image J. Each bar represents ± SD, statistical analysis was performed using unpaired t test (*P<0.05, **P<0.01, ***P<0.001 compared to WT-ER control).

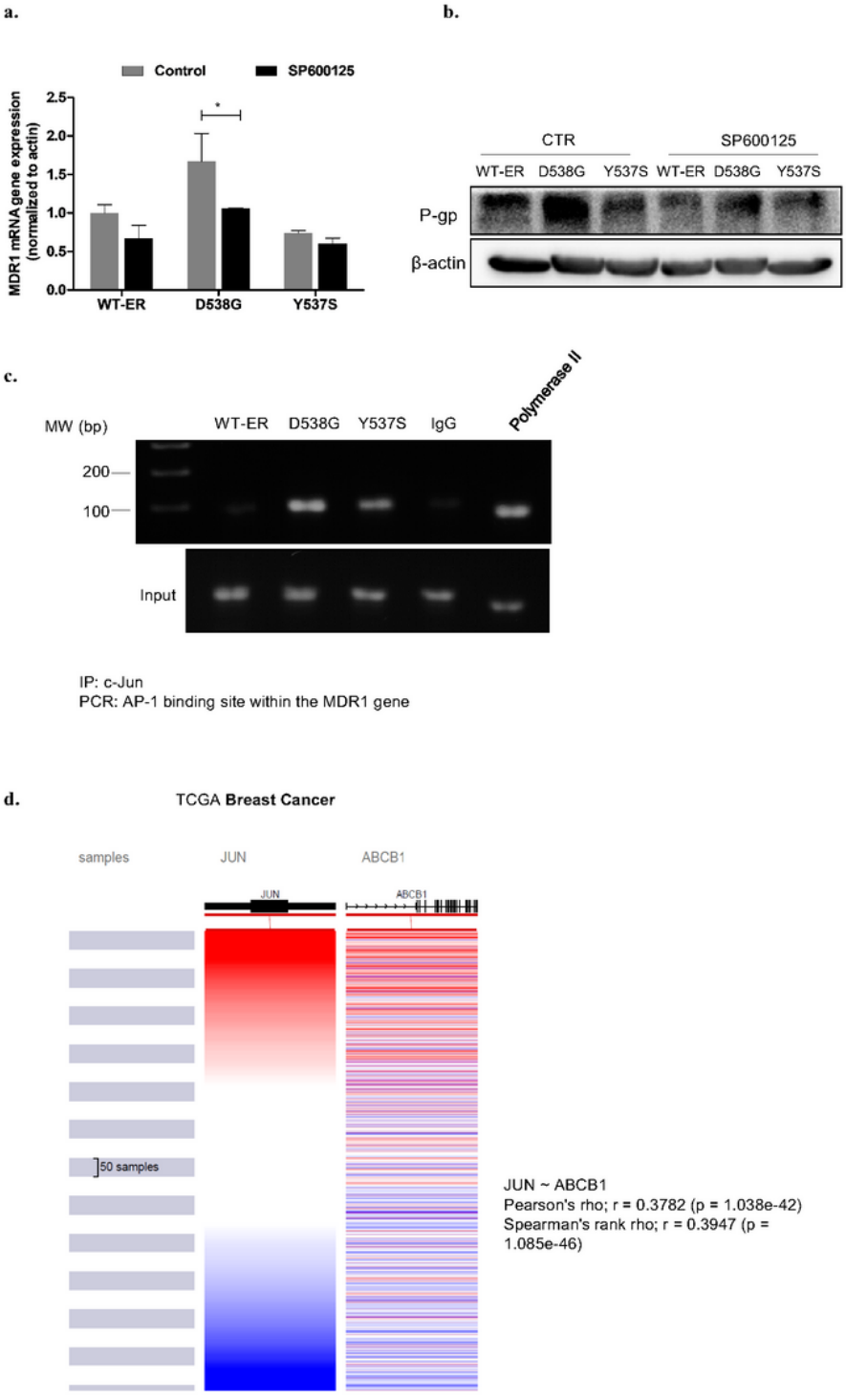

Figure 6

JNK/c-Jun pathway regulates MDR1 expression in mut-ER cells.

(a) WT-ER and LBD-ER MCF-7 cells were treated with 20μM of SP600125 (SP) for 24 hours and the MDR1 mRNA expression level was determined by q-RT-PCR. Values were normalized to β-actin. (b) Expression of P-gp was determined by western blot. (c) ChIP analysis with anti c-Jun antibody for immunoprecipitation was carried out with primers for the AP-1 site on the MDR1 promoter. Normal rabbit IgG was used as a control. (d) Correlation analysis between ABCB1 and JUN gene expressions in breast cancer was conducted using BRCA TCGA dataset, using Xena browser. Correlation analysis was performed using Pearson's and Spearman's correlation. (Red represents high expression of gene, blue represents low expression of gene).

*P<0.05. Each bar represents the mean ± S.D. Experiment was repeated 3 times and a representative experiment is depicted.

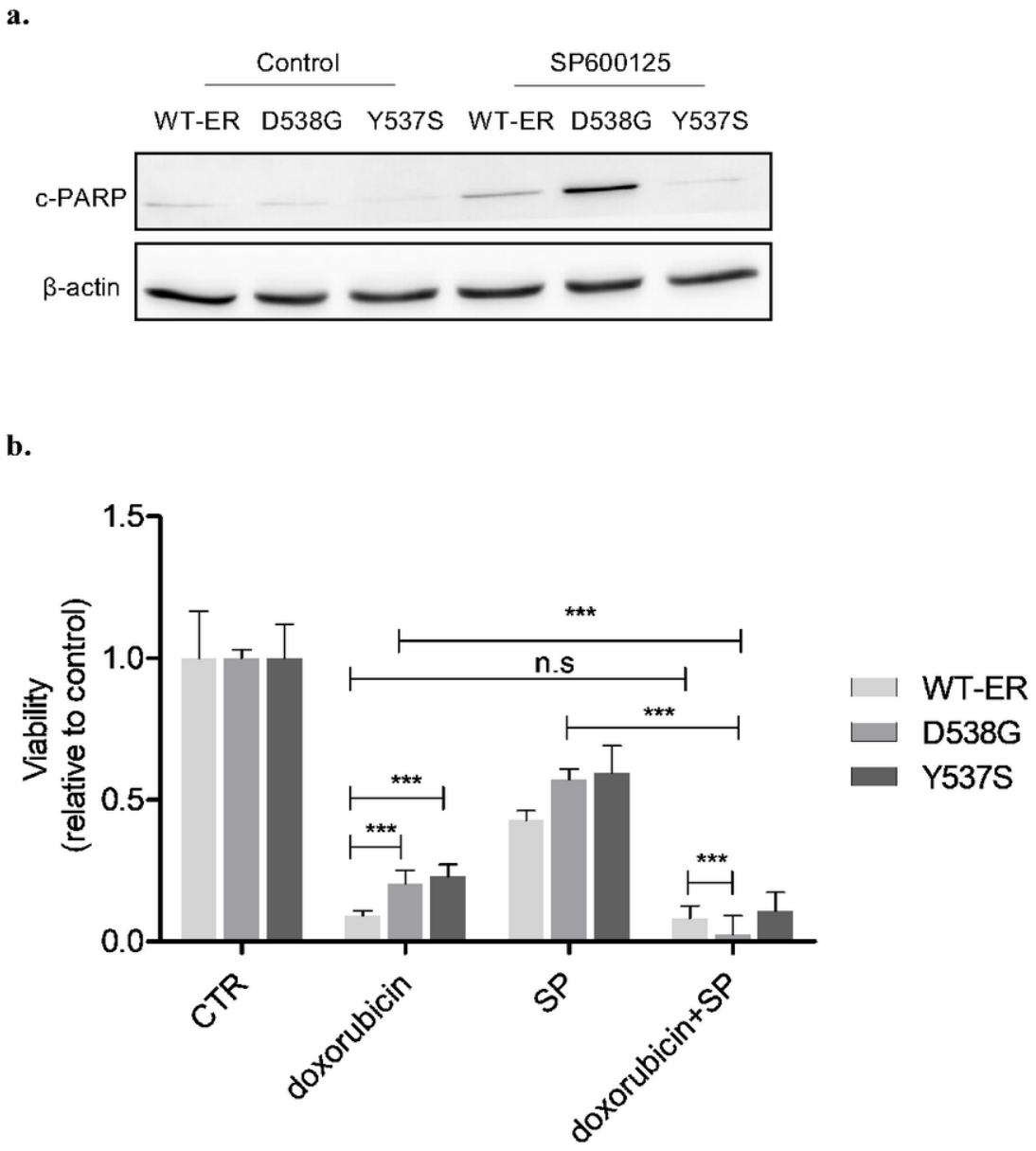

Figure 7

JNK inhibition restores sensitivity of mut-ER and WT-ER cells.

(a) WT-ER and LBD-ER MCF-7 cells were treated with 20μM of SP for 24 hours, then cells were lysed and immunoblotted against c-PARP and β-actin served as a loading control. (b) Cells were seeded in 96 well plates and treated with 20μM SP, 0.5μM doxorubicin, or combination for 72 hours. Viability was assessed using methylene blue assay.

*P<0.05, **P<0.01, ***P<0.001. Each bar represents the mean ± S.D. Experiment was repeated 3 times and a representative experiment is depicted.

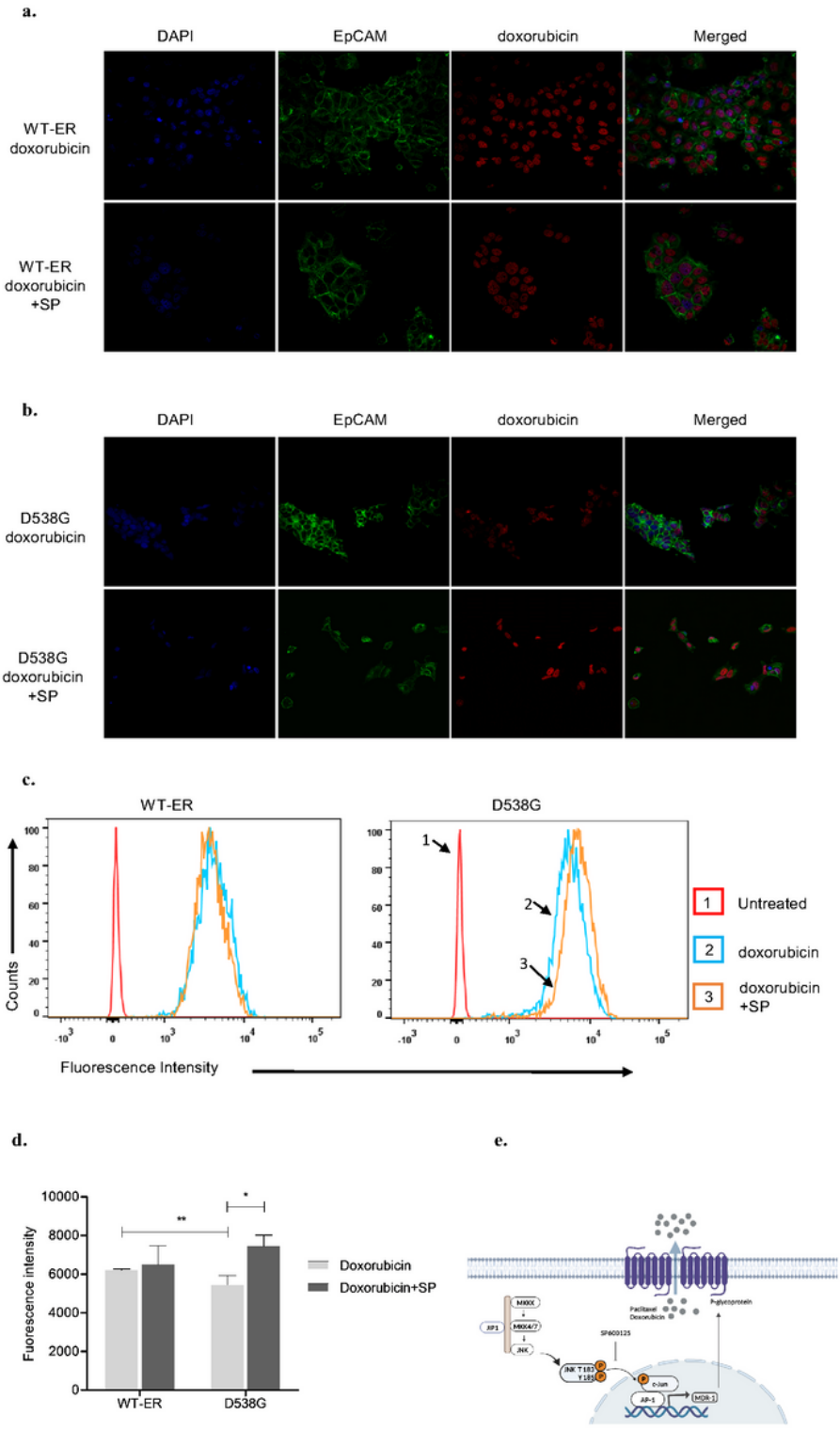

Figure 8

The intracellular accumulation of doxorubicin is decreased in the D538G mutated cells.

Confocal fluorescence microscopy was used to evaluate the intracellular accumulation following the treatment of 10 μM doxorubicin alone and in combination with 20 μM SP for 3 hours in WT-ER (a) and D538G (b). Representative images of DAPI, EpCAM, doxorubicin, and merged are shown. Scale bars represent 100 μm. (c) WT-ER and D538G cells were treated with 10 μM doxorubicin alone and with 20 μM SP for 24 hours. For flow cytometry measurement, cells were trypsinized, diluted in PBS, and analyzed by FACS. (d) Results are shown as the relative mean fluorescence and represent the average of three independent experiments (mean ± SD). Statistical analyses were conducted using the Student's t-test. *P<0.05.

(e) A schematic representation of the JNK/c-Jun MDR1 signaling pathway in the mut-ER cells

Supplementary Files

This is a list of supplementary files associated with this preprint. Click to download.

- Supplementarydata.doc
- articleSuppfigures.ppt